OAK RIDGE INSTITUTE FOR SCIENCE AND EDUCATION
Managed by ORAU for DOE

GENERAL ATOMICS

M3D-C^1 simulations of plasma response in ELM-mitigated AUG and DIII-D discharges

B.C. Lyons[1,2], N.M. Ferraro[2], S.R. Haskey[3], N.C. Logan[3]

[1] Oak Ridge Institute for Science and Education
[2] General Atomics
[3] Princeton Plasma Physics Laboratory

Meeting of the SciDAC Center for Extended MHD Modeling
Savannah, GA
November 15th, 2015

Acknowledgments

- **DIII-D study**
  - Data analyzed largely by C. Paz-Soldan and is the subject of a forthcoming paper
    - "Equilibrium drives of the low and high field side n=2 plasma response and impact on global confinement"
    - To be submitted to *Nuclear Fusion*
  - MARS-F modeling performed by S.R Haskey
  - IPEC modeling performed by N.C. Logan
- **ASDEX-Upgrade data analyzed largely by W. Suttrop**

Introduction

- **External three-dimensional magnetic perturbations have become a principal means of mitigating or suppressing edge-localized modes (ELMs) in tokamaks**
- **Sophisticated magnetohydrodynamics (MHD) modeling is required to understand how the plasma responds to these perturbations**
- **M3D-C^1 is used to model the plasma response in a variety of plasma and magnetic perturbation configurations**
  - Phasing (differential phase angle) between multiple coils
  - Variations in pressure and current profiles
- **Results compared to**
  - Experimental data and observations
  - Numerical results from IPEC and MARS-F

ELMs can be mitigated or suppressed by external 3D magnetic fields

- **DIII-D has demonstrated complete suppression of ELMs using externally-applied 3D magnetic perturbations**
  - Evans, T.E. et al. Nat. Phys. **2**, 419 (2006).
  - Among others
- **Results motivated installation of coils on several machines**
  - ASDEX Upgrade
  - KSTAR
  - MAST
  - NSTX-U
  - ITER (planned)

Theoretical understanding is still incomplete

- **Early theoretical work focused on the nature of the applied vacuum field**
  - Resonant perturbations at rational surfaces open islands
  - Overlapping of islands at edge-pedestal boundary produces stochastic fields
  - Increased transport in stochastic layer maintains pedestal height/ width below ELM stability thresholds
- **Recent MHD simulations have demonstrated the importance of the plasma response**
  - Ideally, resonant fields are completely shielded by plasma currents
  - Resistively, resonant fields can be enhanced by tearing
  - Non-resonant fields excite kink-like deformations with m>nq
  - Kink and tearing structures can couple to each other

Plasma response can greatly alter perturbed magnetic spectrum

- **SURFMN-like field decomposition** $\delta B_r(\psi) = \sum_{m,n} B_{mn}(\psi) \exp\left[i\left(m\theta - n\phi\right)\right]$
- **Resonant response at rational surfaces (m=nq)**
  - Tearing enhances
  - Screening suppresses
- **Kink response amplifies non-resonant fields with m>nq**

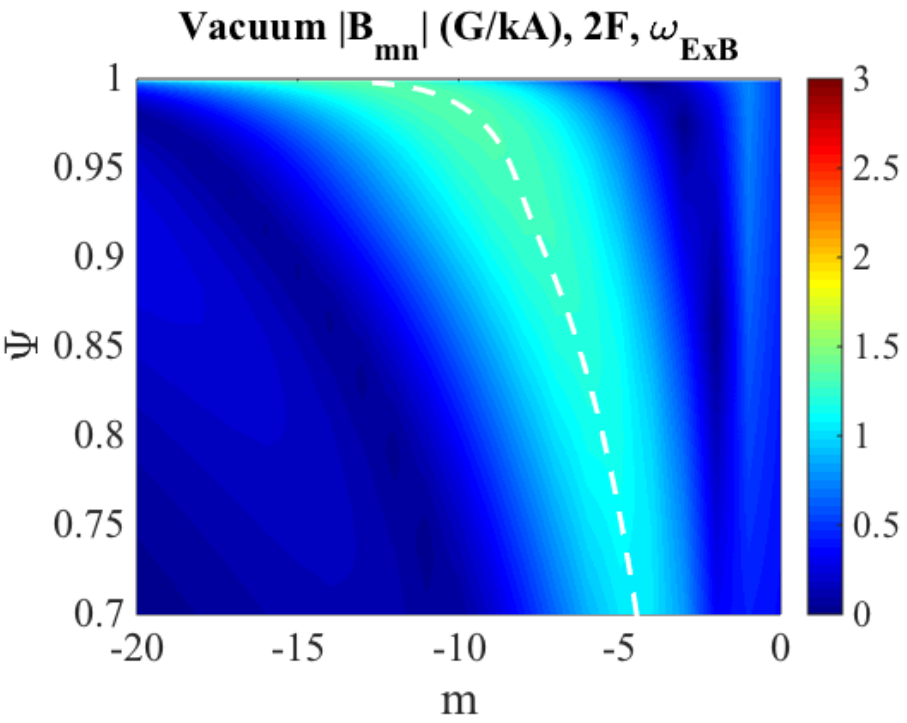

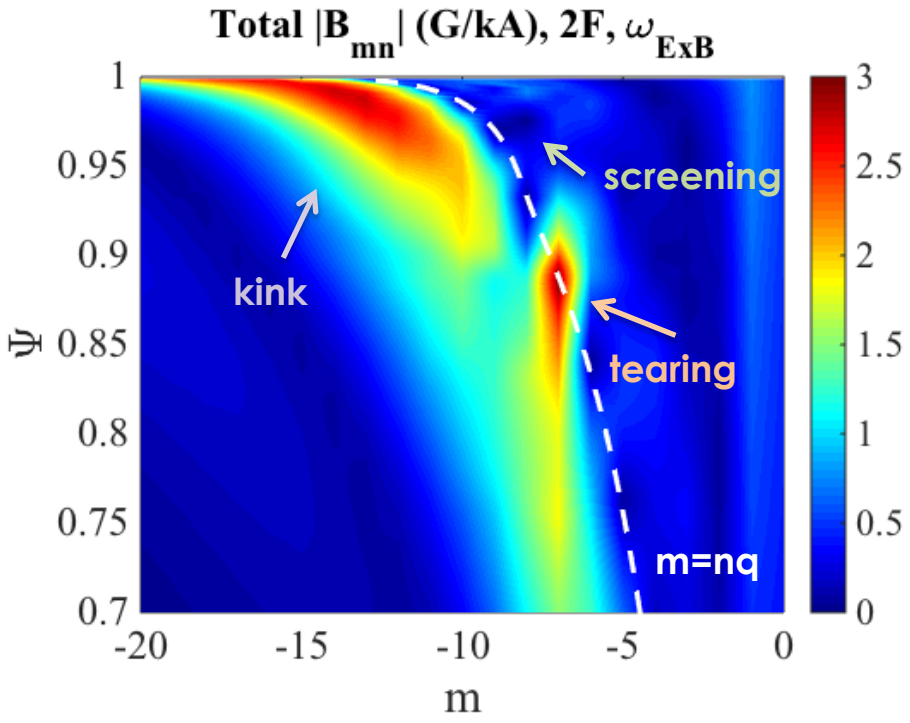

Ideal and resistive MHD modeling capture some, but not all trends

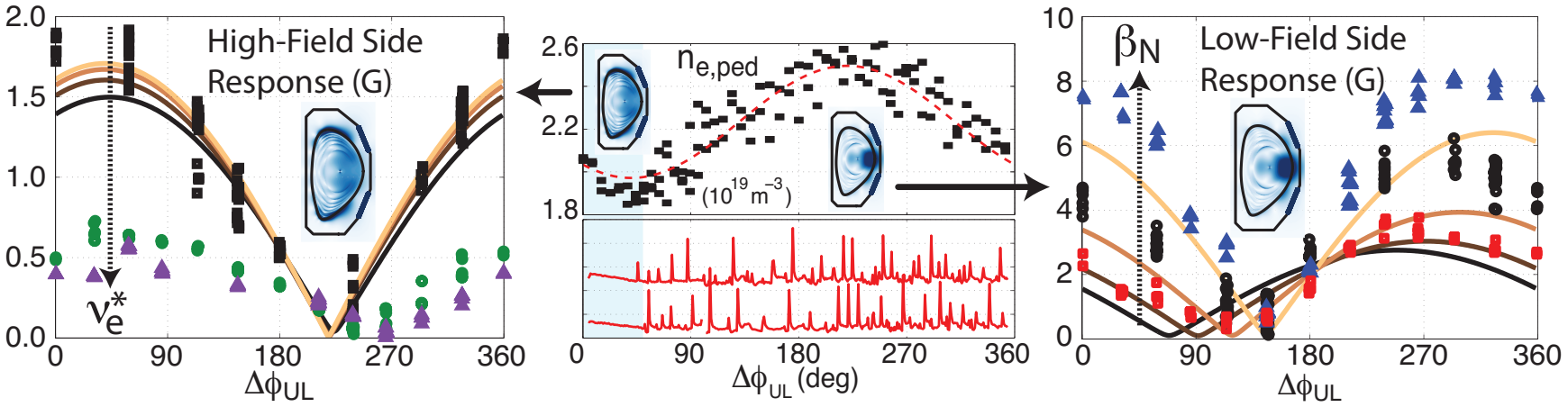

- **IPEC (solid lines) and MARS-F modeling versus data from magnetic probes (symbols)**
  - Generally captures trends as pressure is varied (far right)
  - Struggles to reproduce trends as current profile is varied (far left)
- **Can extended MHD modeling with M3D-C^1 reproduce or improve these results?**

M3D-C^1 allows for extended MHD simulations of the plasma response to applied 3D fields

- **M3D-C^1 [1] is a sophisticated extended MHD code**
  - Fully three-dimensional
  - Two-fluid
  - Linear and nonlinear modes
  - EFIT Grad-Shafranov equilibrium recomputed on adaptive mesh with high-order finite element representation
- **Plasma response calculations**
  - Linear (single toroidal mode number)
  - Time-independent
  - Single- and two-fluid
    - Mostly single-fluid here
  - Experimental kinetic & rotation profiles
    - Extended beyond separatrix
  - Resistive wall model

[1] S. C. Jardin, et al., Comput. Sci. Discovery 5, 014002 (2012).

DIII-D Reference Equilibrium

158103.03796

External field coils on DIII-D

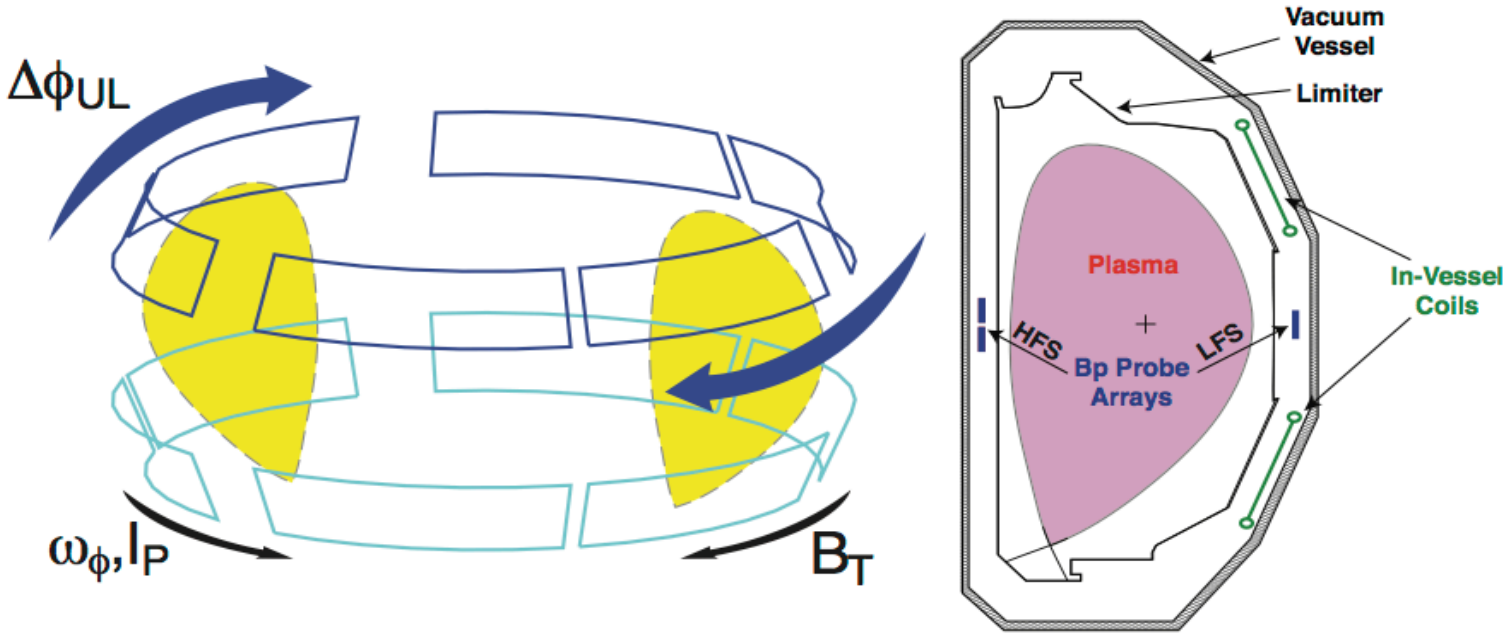

- **Three rows of six saddle coils**
  - Two in-vessel rows (I-coils)
  - One external row (C-coils, not pictured)
  - Toroidal mode number of perturbations up to n=3
- **For n=2 fields, phasing $\Delta\phi_{UL} = \phi_{up} - \phi_{low}$ can be varied between upper and lower coils sets**

Reference is ITER-similar shape, lower single null plasma

- **Reference equilibrium (shot 158103 at 3796 ms) has**
  - $B_T = 1.93$ T and $I_P = 1.36$ MA
  - $\beta_N = 2.2$
  - $\nu_{e^*} = 0.3$
  - $q_{95} = 4.15$
- **n=2 external 3D field applied with I-coils**
  - Relative phase (phasing) between upper and lower coil changed in piecewise fashion
  - Phase of both coils flipped throughout shot for diagnostic purposes

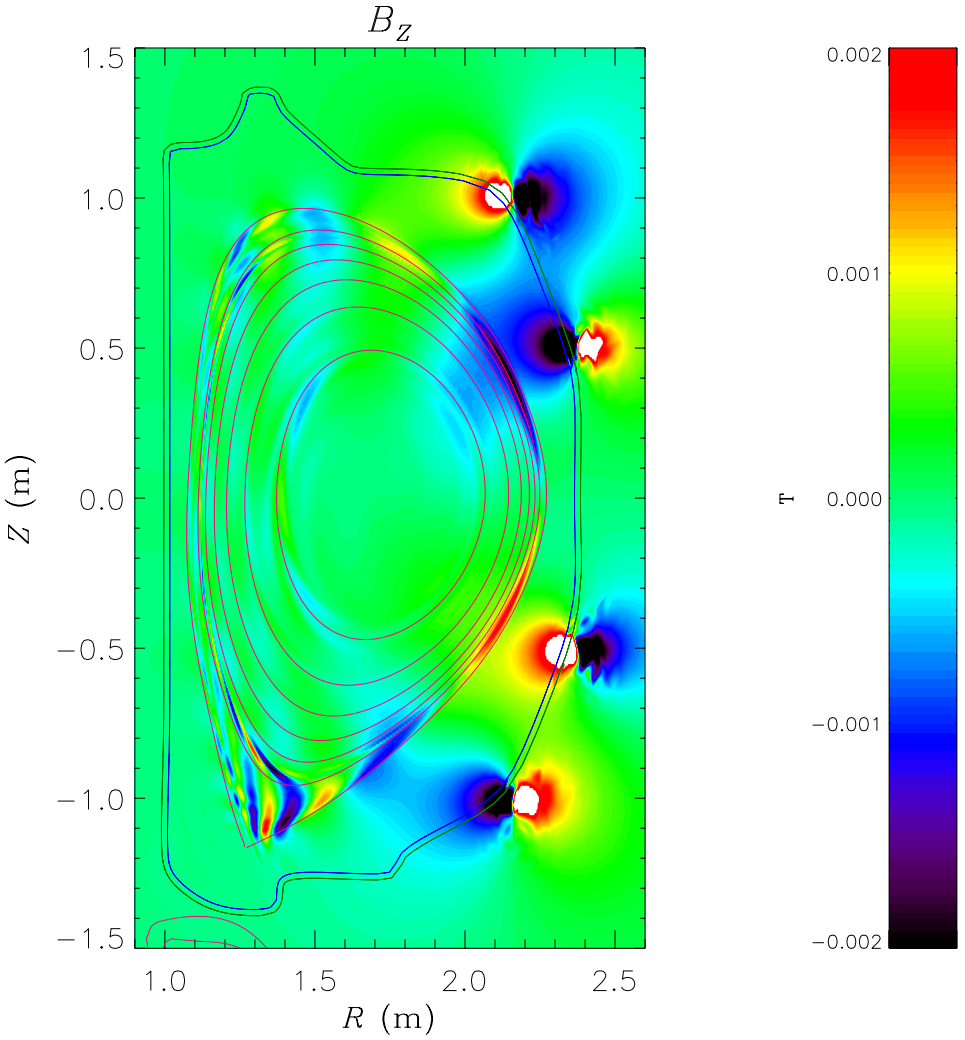

LFS and HFS magnetic response measurements show multimode response on DIII-D

- **These plots show**
  - Magnitude of perturbed magnetic field as the phasing is varied
  - Signal at low-field side (LFS) and high-field side (HFS) probes
  - Field from plasma response only
  - Null occurring where response from upper and lower coils cancels
- **Signals at LFS and HFS have different phasing dependences**
- **Indicates multiple modes are being driven simultaneously in DIII-D with n=2 fields**
- **For more detail, see C. Paz-Soldan et al., PRL 114, 105001 (2015)**

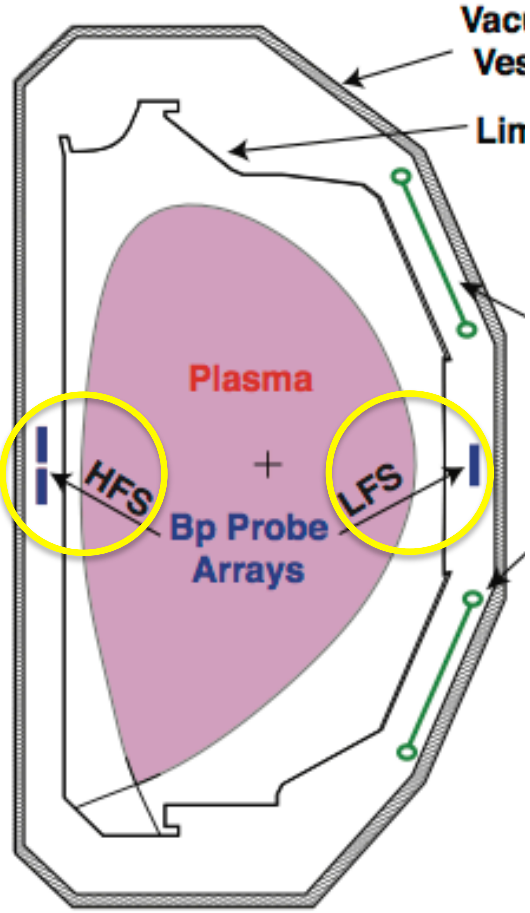

LFS and HFS magnetic response measurements show multimode response on DIII-D

- **These plots show**
  - Magnitude of perturbed magnetic field as the phasing is varied
  - Signal at low-field side (LFS) and high-field side (HFS) probes
  - Field from plasma response only
  - Null occurring where response from upper and lower coils cancels
- **Signals at LFS and HFS have different phasing dependences**
- **Indicates multiple modes are being driven simultaneously in DIII-D with n=2 fields**
- **For more detail, see C. Paz-Soldan et al., PRL 114, 105001 (2015)**

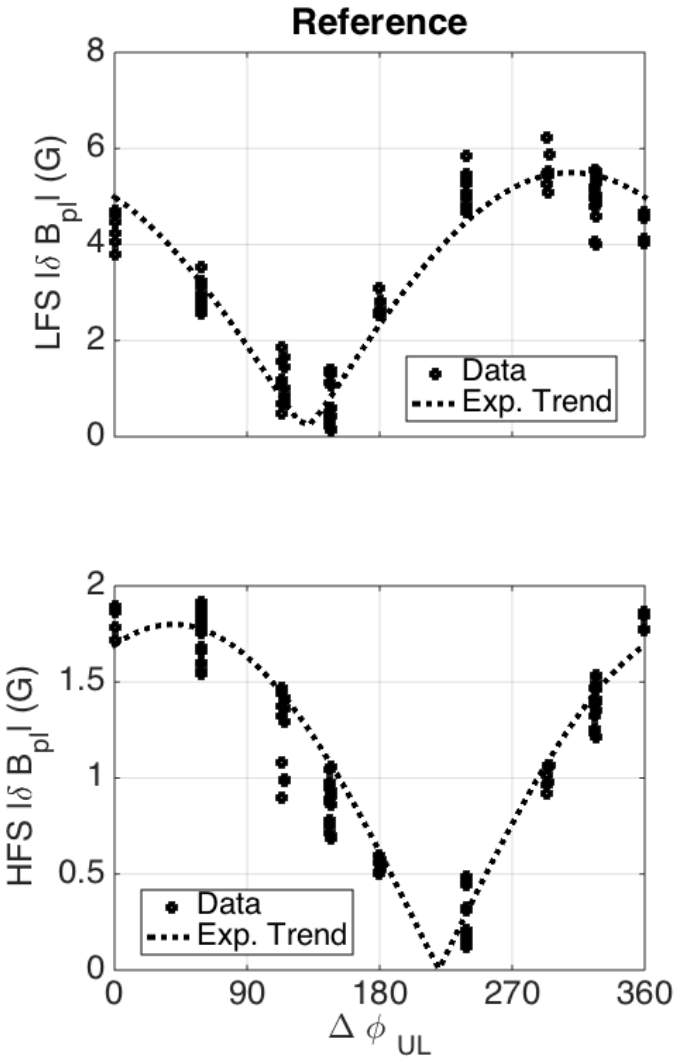

Modeling of reference shows excellent agreement between experimental data and various codes

- **IPEC[1] uses an ideal MHD model**
  - No rotation
  - Perfect screening at rational surfaces
- **MARS-F[2] uses a single-fluid, resistive MHD model**
  - Simulations performed with carbon toroidal rotation profile
  - Resistivity allows for tearing or imperfect screening
- **Here, M3D-C[1] use single-fluid model with ExB rotation profile**

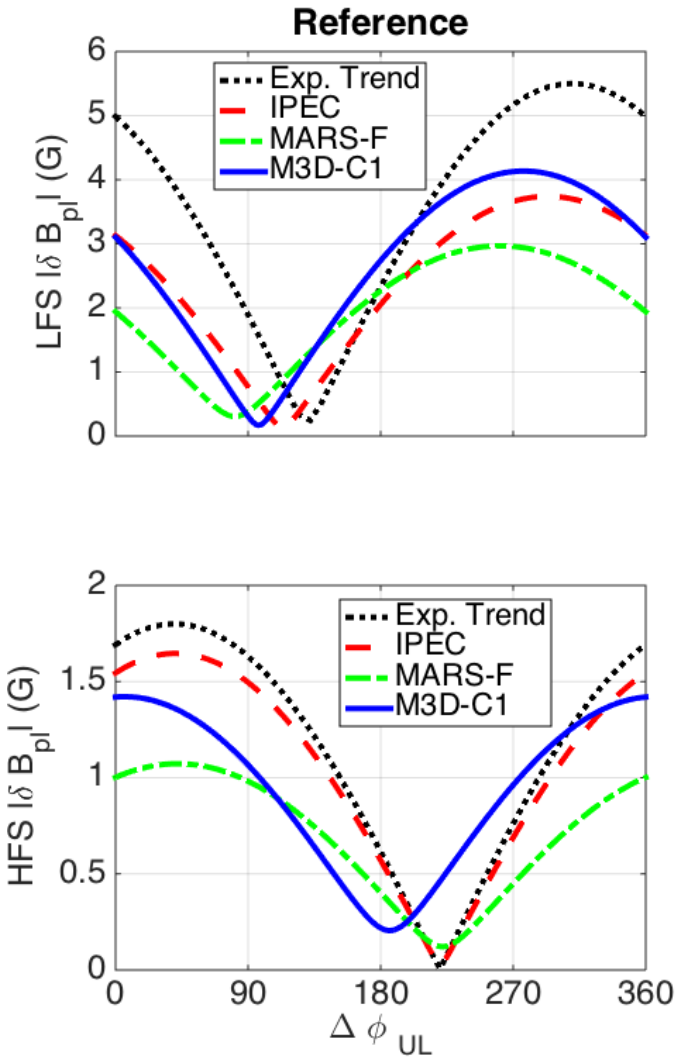

[1] J.-K. Park, A.H. Boozer, and A.H. Glasser, Phys. Plasmas 14, 052110 (2007).

[2] Y. Q. Liu, et al., Phys. Plasmas 7, 3681 (2000).

M3D-C^1 results sensitive to changes in non-ideal effects

Using carbon toroidal rotation improves agreement with MARS-F

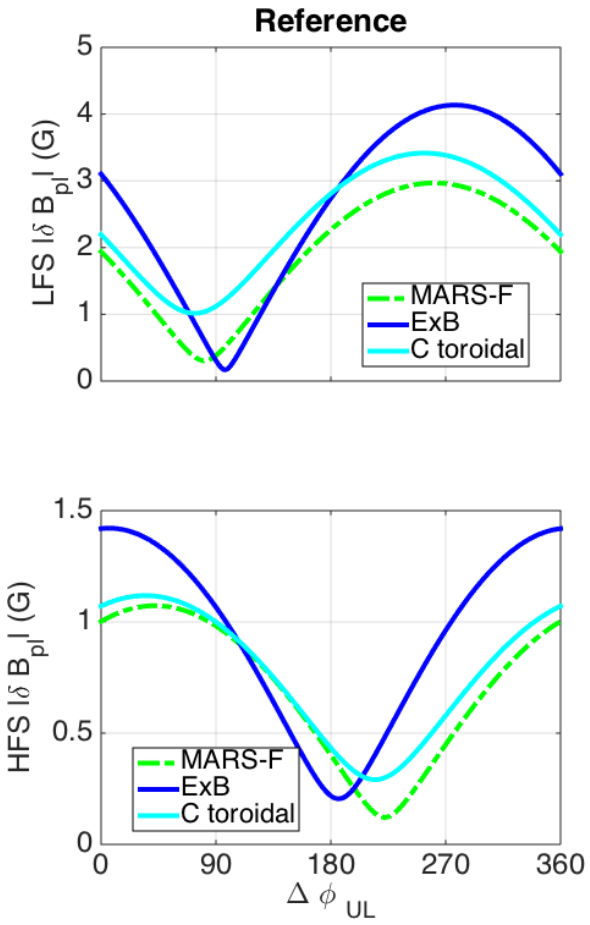

Including two-fluid terms gives poorer agreement with data

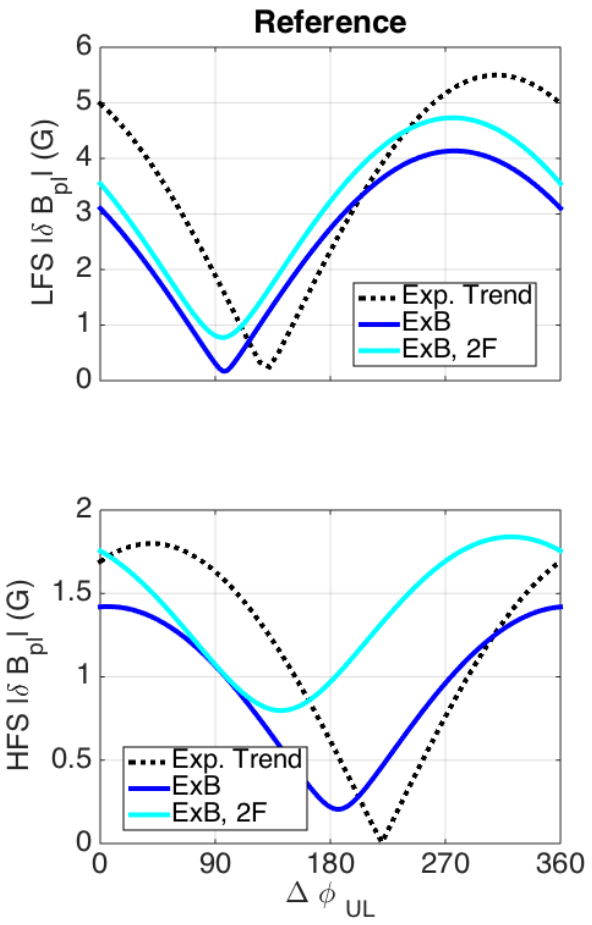

Carbon toroidal rotation profile results in reduced kink response

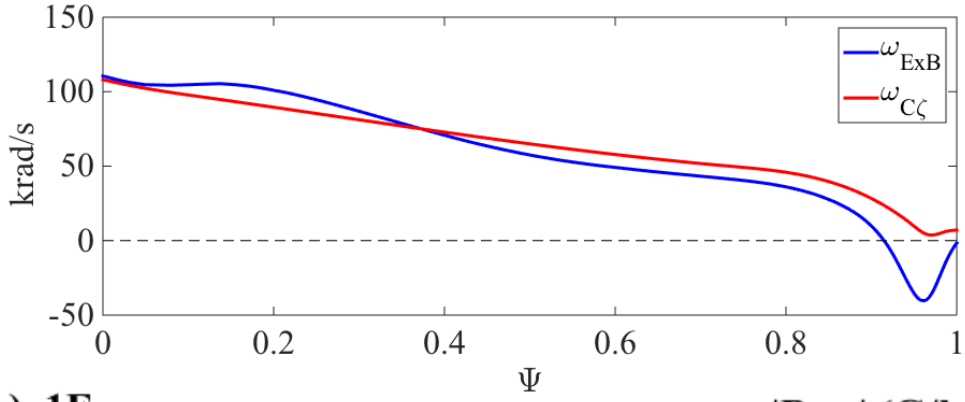

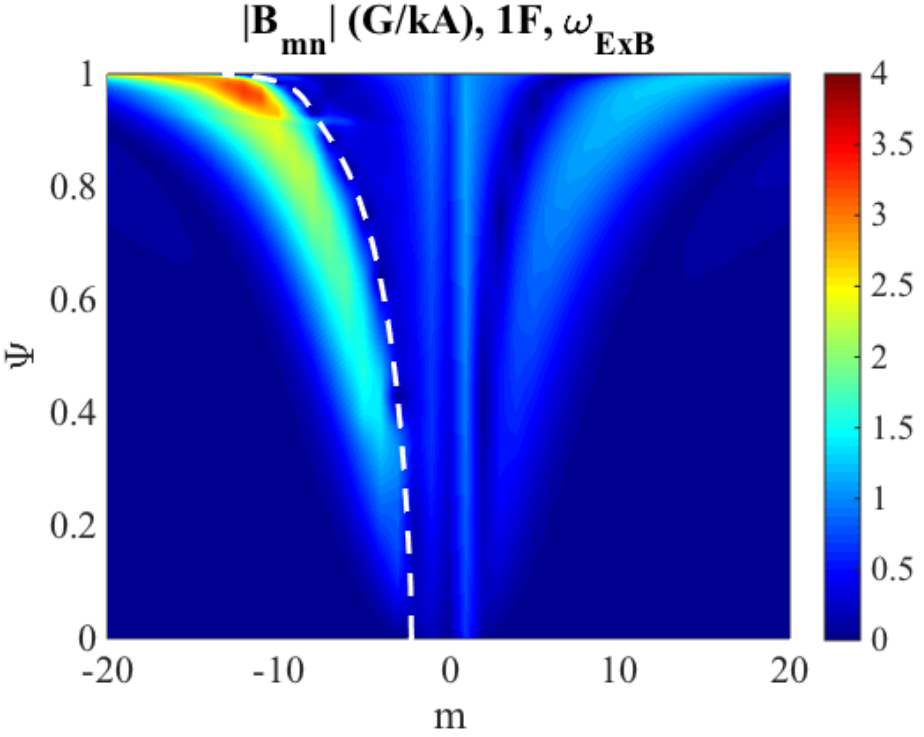

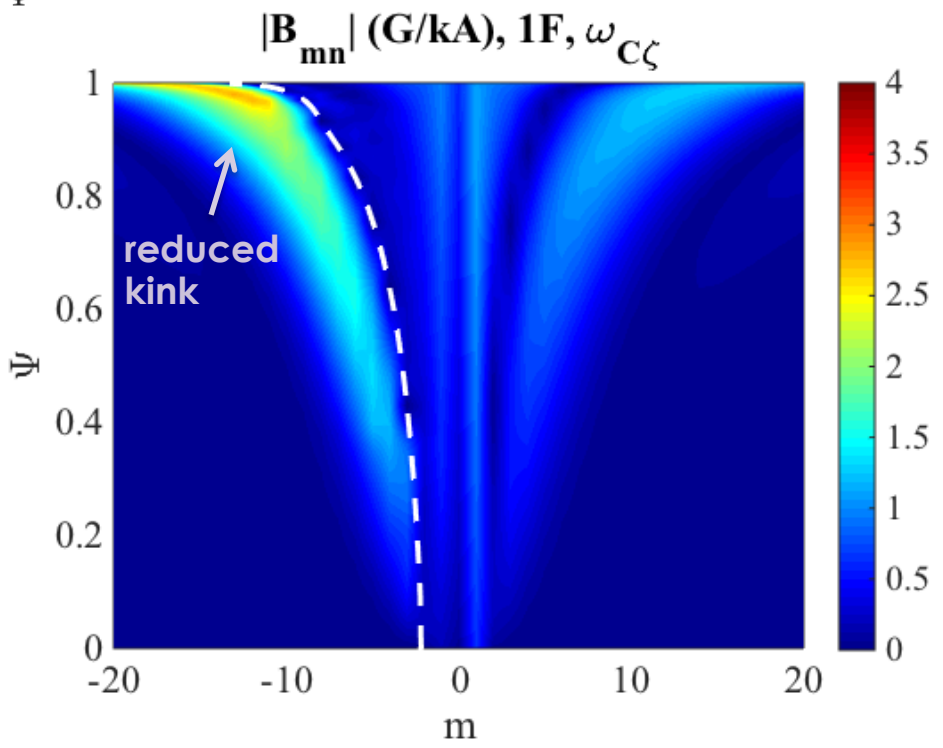

Enhanced tearing in two-fluid simulation due to electron rotation zero crossing near q=7/2

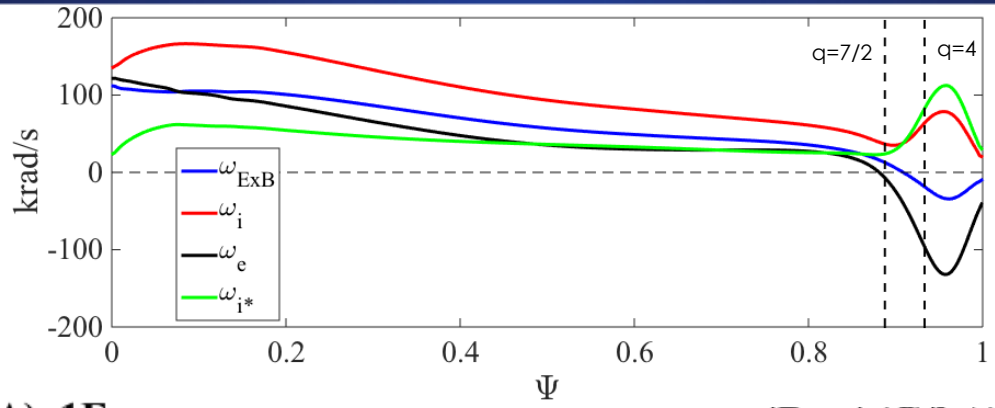

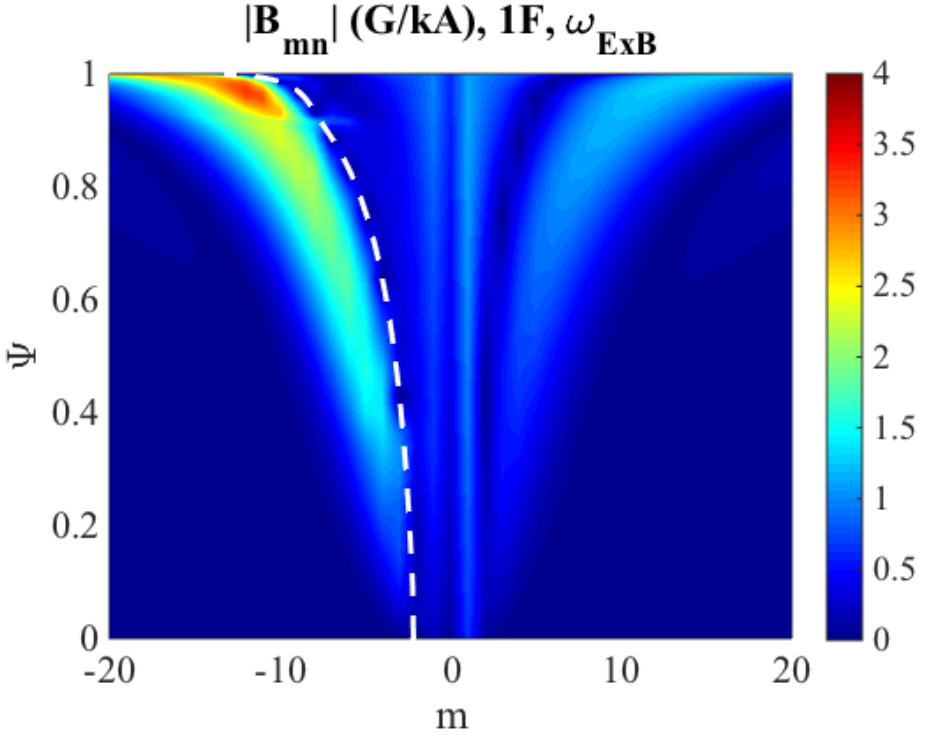

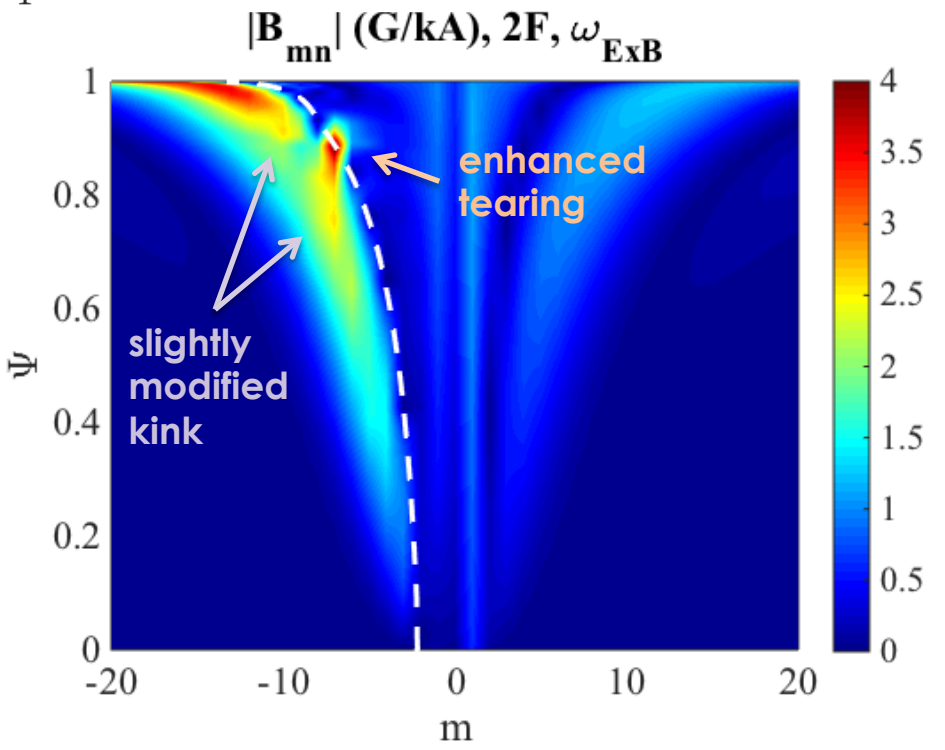

Plasma response variation with equilibrium parameters

High q95 trends on both LFS and HFS roughly captured by M3D-C¹ modeling

- **High q95 discharge has**
  $q_{95} = 5.1$ $\beta_N = 2.2$ $\nu_{e*} = 0.25$
- **LFS probe shows slight shift in phasing variation**
- **HFS probe shows significant amplitude decrease**
- **M3D-C¹ sees both these trends, although**
  - LFS phase shift somewhat larger than experiment
  - HFS amplitude decrease somewhat smaller than exp.
- **IPEC and MARS-F find phase shift on LFS but don't capture amplitude reduction on HFS**

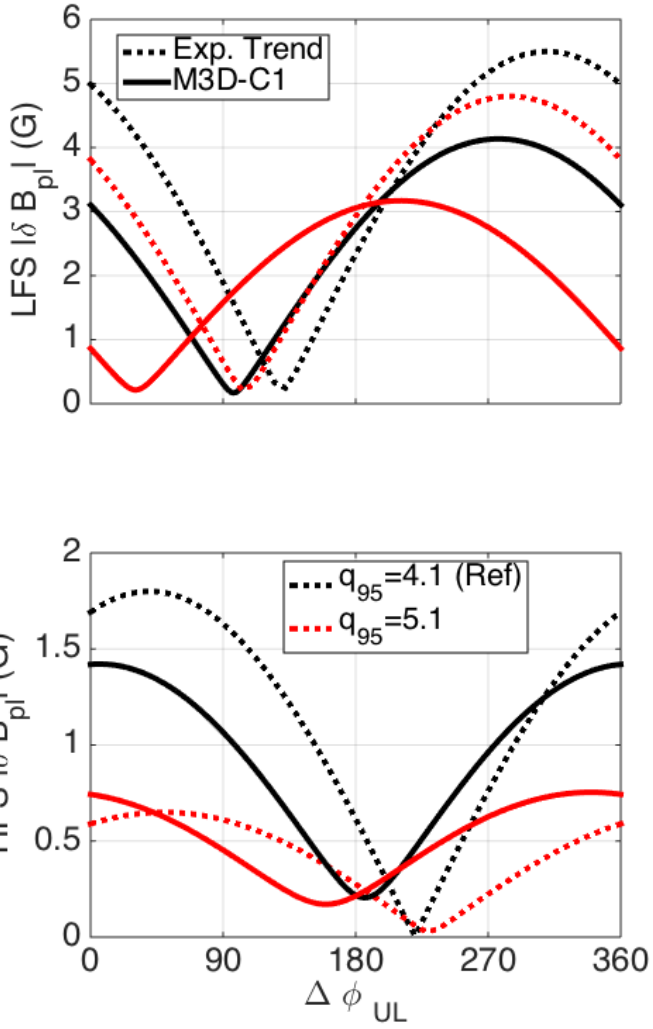

H- to L-mode trends on both LFS and HFS captured by M3D-C^1 modeling

- **L-mode discharge has**
  $q_{95} = 3.8 \quad \beta_N = 0.50 \quad \nu_{e*} = 15$
- **LFS probe shows**
  - significant amplitude decrease
  - large shift in phasing variation
- **HFS probe shows**
  - significant amplitude decrease
  - slight shift in phasing variation
- **L-mode closer to single-mode response**
- **M3D-C^1 sees these trends, though the amplitude decreases are somewhat smaller**
- **IPEC and MARS-F capture LFS but not HFS trends**

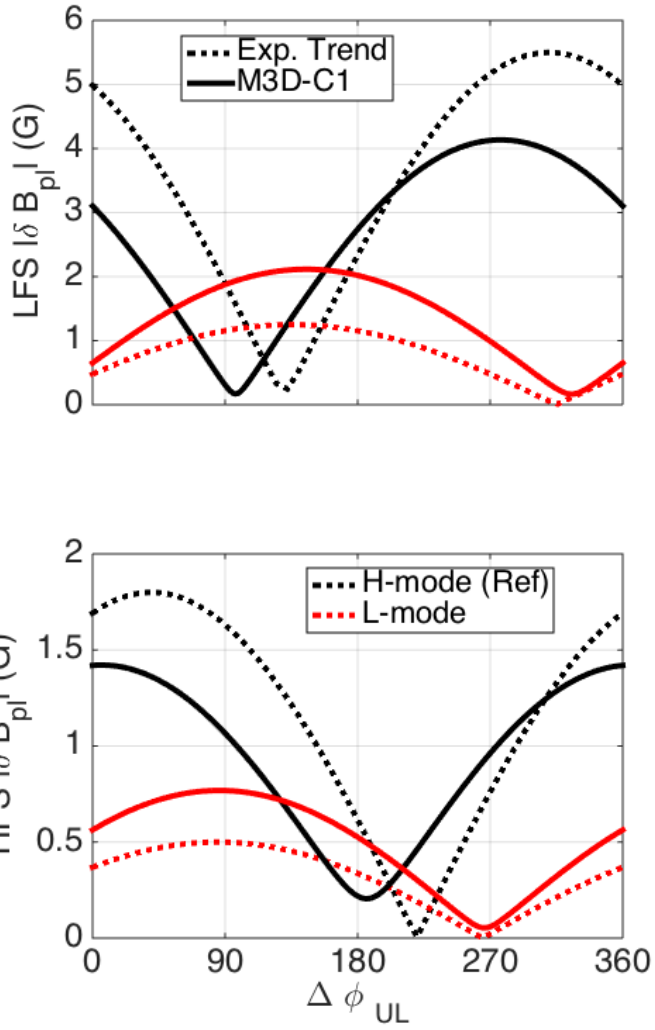

M3D-C^1 struggles to reproduce β trends

- **Low-β discharge**
  $\beta_N = 1.3$ $\nu_{e*} = 0.3$ $q_{95} = 4.05$
- **High-β discharge**
  $\beta_N = 2.8$ $\nu_{e*} = 0.15$ $q_{95} = 4.25$
- **LFS probe shows**
  - significant amplitude increase
  - slight phasing shift w/ increasing β
- **HFS probe response largely insensitive to β**
- **M3D-C^1 modeling**
  - Does an okay reproducing LFS trend, especially at highest β
  - Does not capture HFS invariance
- **IPEC captures both trends for smoothly-varied equilibria**

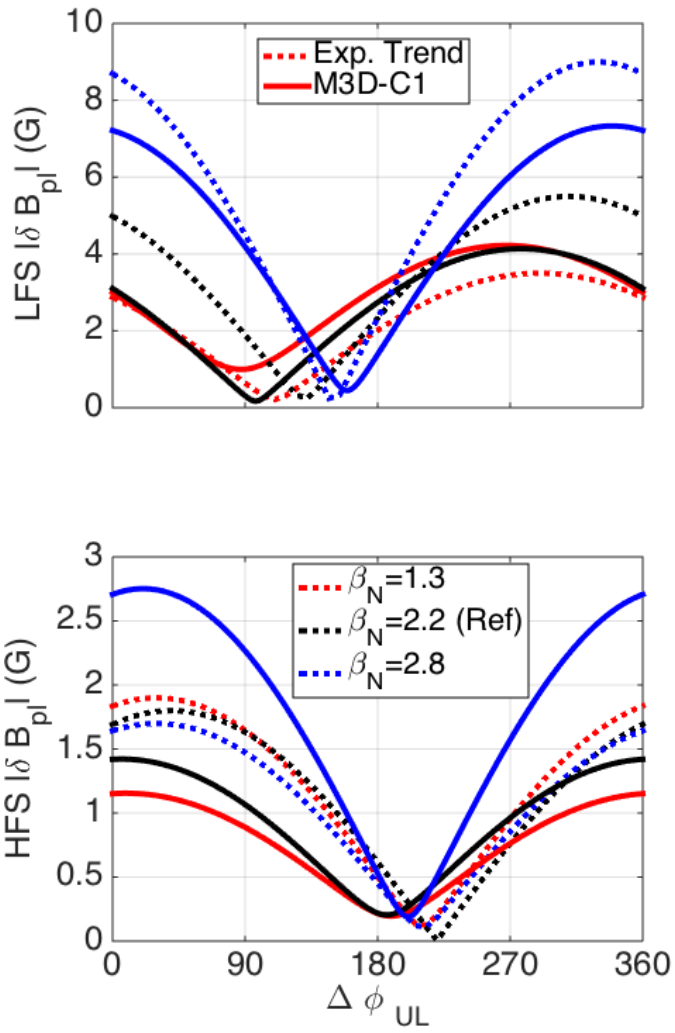

ASDEX Upgrade

External field coils on ASDEX Upgrade

- **Two rows of eight in-vessel saddle coils**
- **Toroidal mode number of perturbations up to n=4**
- **For n=2 fields, the differential phase angle (AKA phasing) can be varied between upper and lower coils sets**
  - $\Delta\varphi = \phi_{up} - \phi_{low}$
  - Varies the magnetic pitch angle of the applied field
  - Affects coupling of resonant and non-resonant fields

Figure 1 from G D Conway et al 2015 Plasma Phys. Control. Fusion 57 014035

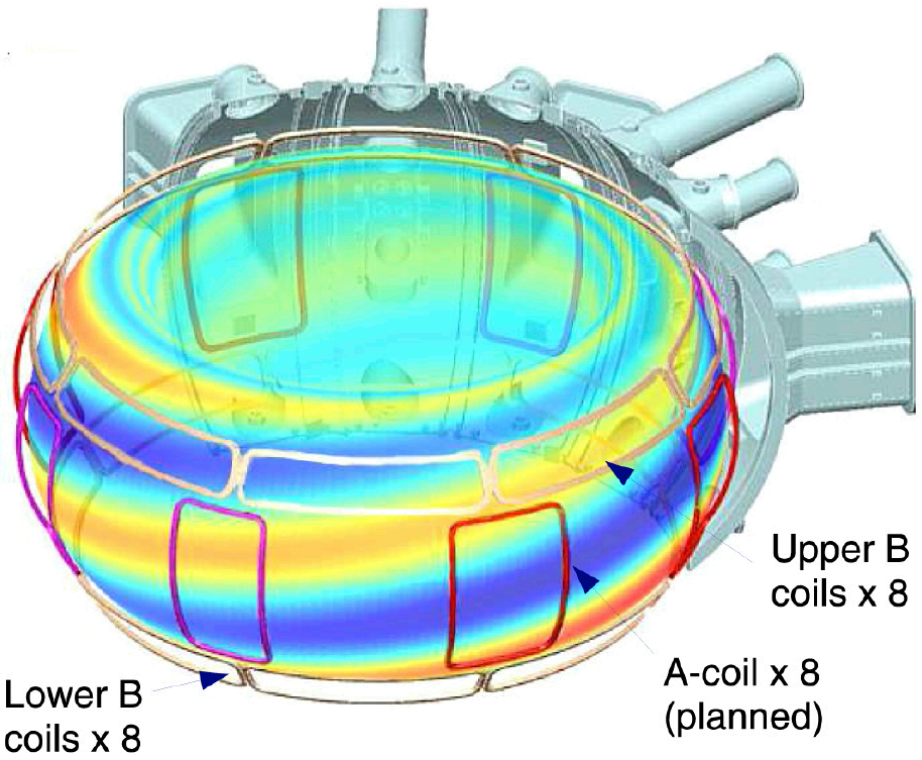

Phasing affects the magnitude of ELM mitigation

- **Density and ELM frequency are modulated by phasing**
- **Strongest mitigation at minimum density**

Suttrop, W. et al. EX/P1-23. IAEA FEC 2014.

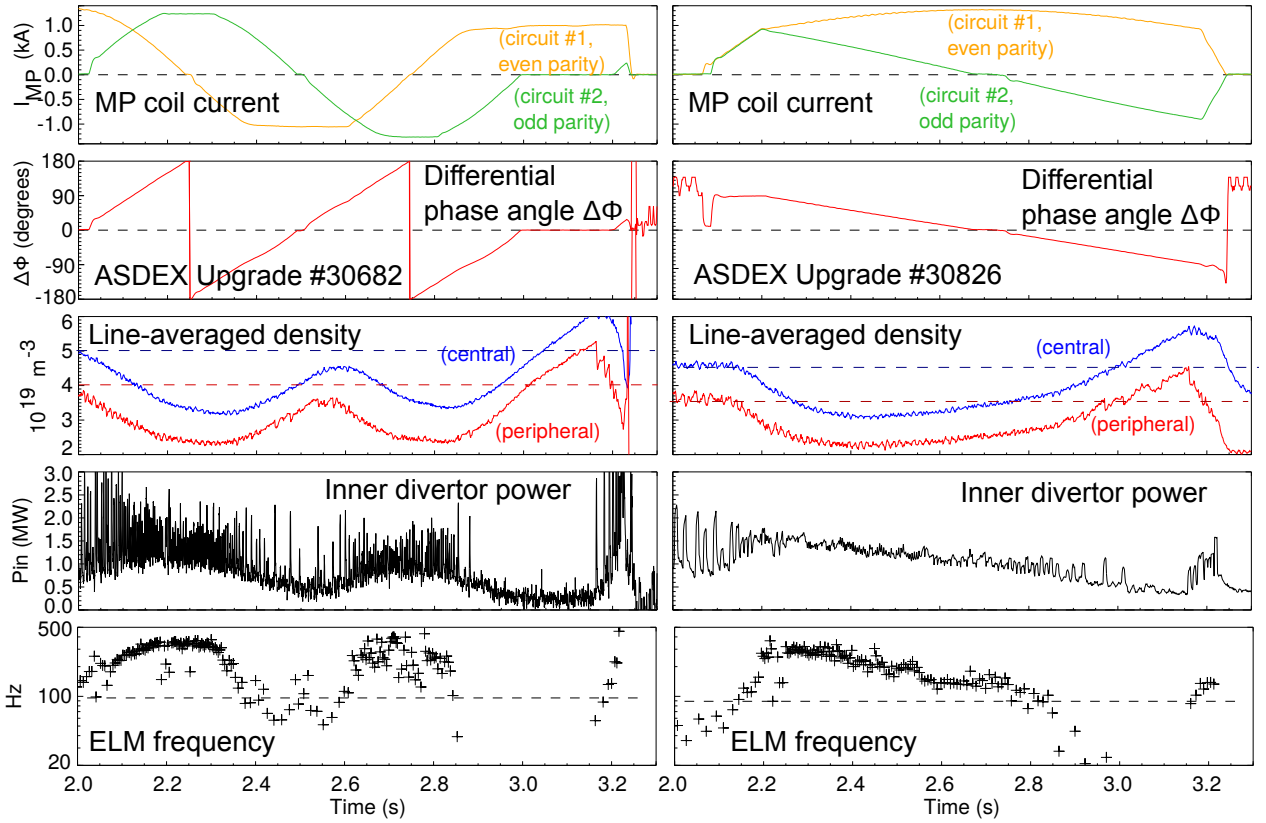

M3D-C^1 has calculated the plasma response for ASDEX Upgrade shot 30835

- **Good ELM mitigation observed with n=2 fields in 30835 and similar shots**
- **Four phasings have been studied with MARS-F and VMEC**
  - $\Delta\varphi = 30°$: Optimum vacuum resonance
  - $\Delta\varphi = 90°$: Strongest ELM mitigation
  - $\Delta\varphi = -90°$: Classical, non-stationary ELM-free phase
  - $\Delta\varphi = -150°$: Optimum non-resonant field (ELM mitigation observed)
- **We've used M3D-C^1 to examine this shot**
  - Time-independent, linear analysis
  - Not quantitative validation work
    - Not comparing to measured field data
    - Only examining qualitative trends/correlations

Resonant and non-resonant fields may both impact ELM mitigation

- **Strongest ELM mitigation occurs where resonant field is maximized**
- **Non-resonant field may play significant role**
  - Resonant field similar at $\Delta\varphi = 30°$ & $\Delta\varphi = -150°$
  - Non-resonant field significantly stronger at $\Delta\varphi = -150°$ where ELM mitigation is observed

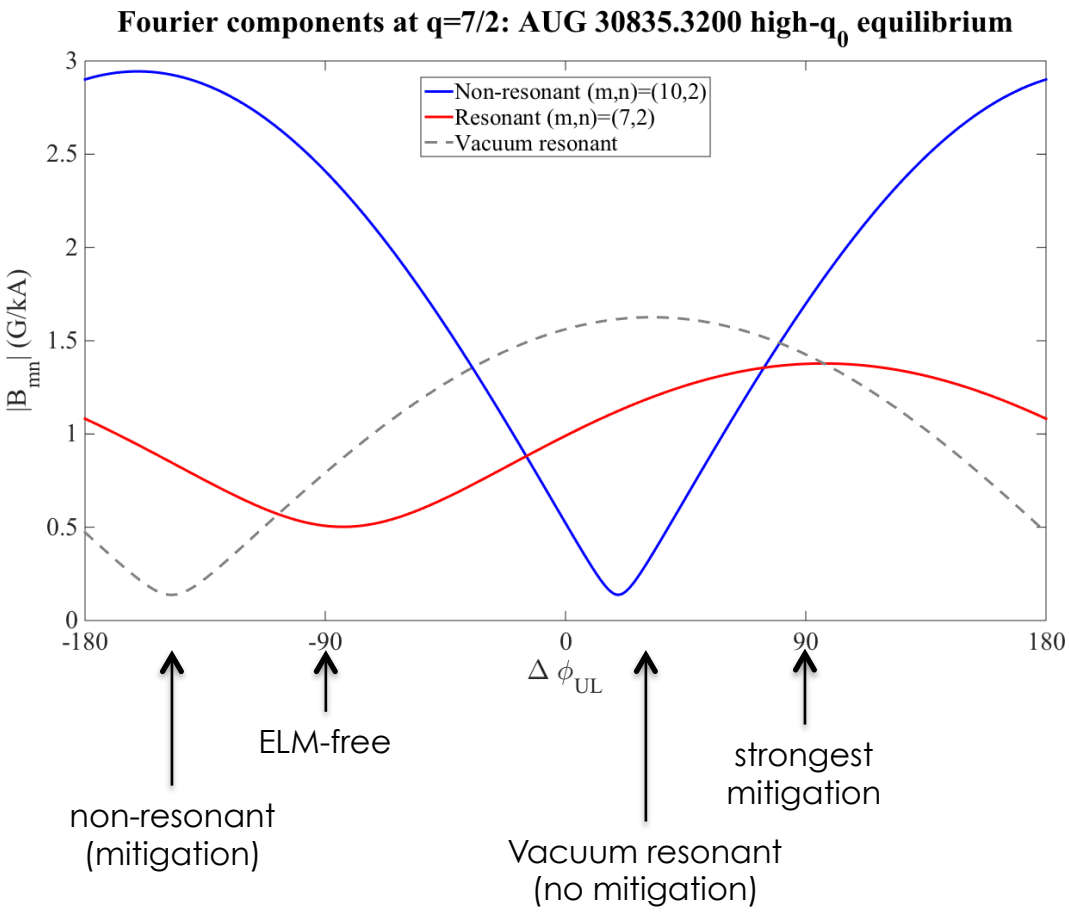

Summary

- **M3D-C^1 has been used to calculate the linear, steady-state plasma response of DIII-D and ASDEX Upgrade to external, three-dimensional magnetic perturbations**
- **Validation against magnetic probe signals on DIII-D shows**
  - Good agreement with reference, L-mode, and high-q_{95} equilibria
  - Poor agreement with data as β is varied
- **Cross-code verification work with IPEC and MARS-F**
  - M3D-C^1 captures some trends on the magnetic probes not captured by IPEC and MARS-F, and vice versa
  - Source of discrepancies in between the codes, and with the data, still uncertain
  - M3D-C^1 modeling demonstrates sensitivity to the rotation profile
    - MARS-F may achieve better agreement with data if ExB rotation profile is used
  - Small changes in the degree of resonant penetration can have relatively large impact on magnetic signals

Summary (continued) and future work

- **Preliminary investigations on ASDEX Upgrade suggest that ELM mitigation is determined by both resonant and non-resonant affects**
- **Future work**
  - Detailed comparison between Fourier spectra from M3D-C^1, IPEC, and MARS-F solutions to determine source of discrepancies
  - Further examination of sensitivities to nonideal effects
    - Rotation profile variation on M3D-C^1 and MARS-F
    - Improved two-fluid analysis with M3D-C^1
  - Additional studies of ASDEX Upgrade plasmas
    - Examine other shots, especially from recent experiments
    - Perform quantitative validation work
  - New collaboration with KSTAR to study ELM suppression experiments, including multiple toroidal harmonics

OAK RIDGE INSTITUTE FOR SCIENCE AND EDUCATION
Managed by ORAU for DOE

GENERAL ATOMICS

Low-collisionality drift-kinetic calculations in up-down asymmetric M3D-C^1 equilibria

B.C. Lyons[1,2], N.M. Ferraro[2], J.J. Ramos[4], S.C. Jardin[3]

[1] Oak Ridge Institute for Science and Education
[2] General Atomics
[3] Princeton Plasma Physics Laboratory
[4]Massachussetts Institute of Technology Plasma Science and Fusion Center

Meeting of the SciDAC Center for Extended MHD Modeling
Savannah, GA
November 15th, 2015

NIES solves to the low-collisionality drift-kinetic distribution function

- **The Neoclassical Ion-Electron Solver (NIES) solves a set of drift kinetic equations (DKEs)**
  - Steady-state distribution function in general, axisymmetric geometries
  - Deep in low-collisionality regime
  - Conductivity, flows, and bootstrap currents can be calculated
  - DKEs reduce to solvability conditions on the linearized Fokker-Planck-Landau collision operator

$$\oint_{\psi,w,\lambda} \frac{dl}{w_{\|}} C_s\left[\varsigma H K_s\right] = -\oint_{\psi,w,\lambda} dl S_s$$

$$\begin{aligned} C_s\left[K_s\right] = & \frac{2\nu_{Ds}(w)}{w}\frac{\partial}{\partial\lambda}\left(\eta_1(\lambda)\lambda\frac{\partial K_s}{\partial\lambda}\right) + \frac{4\pi\nu_s v_{ths}^3}{nw} f_{Ms}\eta_2(\lambda)K_s \\ & + \nu_s\eta_2(\lambda)\frac{v_{ths}^3}{w^3}\frac{\partial}{\partial w}\left[\xi_s\left(w\frac{\partial K_s}{\partial w} + \frac{w^2}{v_{ths}^2}K_s\right) + \xi_{s'}\left(w\frac{\partial K_s}{\partial w} + \frac{m_s w^2}{m_{s'}v_{ths'}^2}K_s\right)\right] \\ & - \frac{\nu_s v_{ths}}{nw} f_{Ms}\int_0^{2\pi}\frac{\mathcal{J}B}{y(\theta,\lambda)}\Phi_s d\theta + \frac{\nu_s w}{n v_{ths}} f_{Ms}\frac{d^2}{dw^2}\int_0^{2\pi}\frac{\mathcal{J}B}{y(\theta,\lambda)}\Psi_s d\theta. \end{aligned}$$

$$\begin{aligned} \mathcal{S}_e = & \left\{\frac{eV_0 I}{T_e}\int_0^{2\pi}\frac{\mathcal{J}}{R^2}d\theta + \frac{\nu_e v_{the}}{v_{thi}^2 w}\xi_i\left(U_i\int_0^{2\pi}\mathcal{J}B^2 d\theta + \frac{I}{en}\frac{dp}{d\psi}\int_0^{2\pi}\mathcal{J}d\theta\right)\right. \\ & \left. + \frac{\nu_e m_e I}{eT_e}\frac{dT_e}{d\psi}\frac{v_{the}}{w}\left[2\varphi_e - 10\xi_e + \frac{1}{2}\varphi_i - \frac{5v_{the}^2}{2v_{thi}^2}\xi_i\right]\int_0^{2\pi}\mathcal{J}d\theta\right\} f_{Me} \end{aligned}$$

$$\mathcal{S}_i = -\frac{\nu_i m_i I}{eT_i}\frac{dT_i}{d\psi}\frac{v_{thi}}{w}\left[2\varphi_i - 10\xi_i\right] f_{Mi}\int_0^{2\pi}\mathcal{J}d\theta$$

NIES can now accept M3D-C^1 equilibria as input

- **Previously NIES used**
  - Analytic, large aspect ratio equilibria
  - Numerical equilibria from JSOLVER
  - Only up-down symmetric equilibria had been considered
- **IDL routines written by N.M. Ferraro output necessary quantities from M3D-C^1 equilibria**
  - Translate equilibria to flux coordinates as used by NIES
  - NetCDF standard output
- **NIES modified to read these equilibria**
  - Initialization subroutines convert NetCDF input to NIES data structures
  - Few other changes needed to NIES

NIES conductivity and bootstrap currents for M3D-C^1 and JSOLVER equilibria benchmarked to Sauter fits

DIII-D equilibrium below is from M3D-C^1

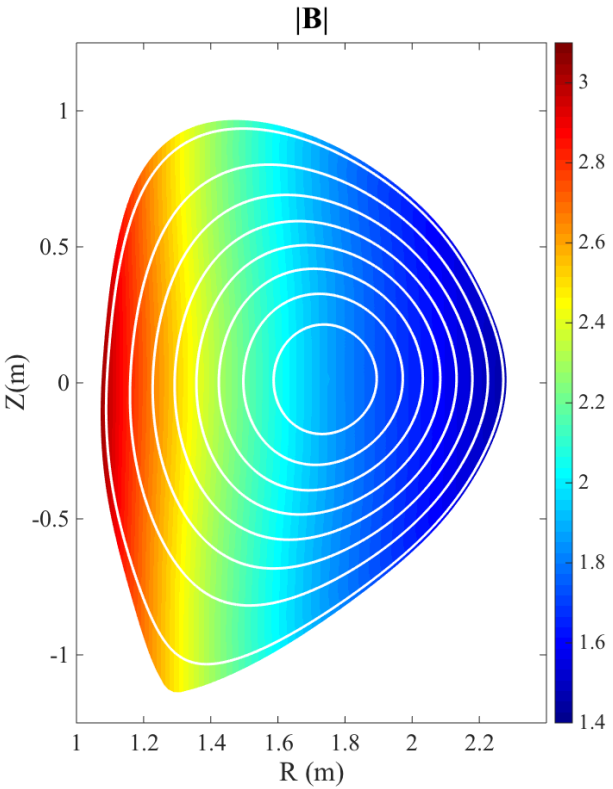

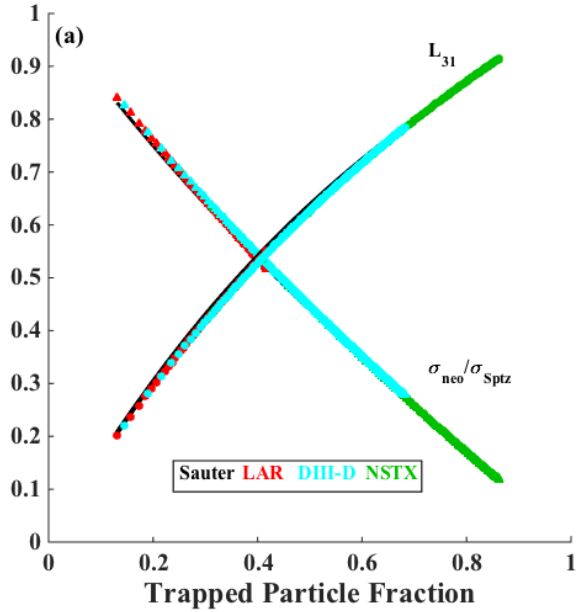

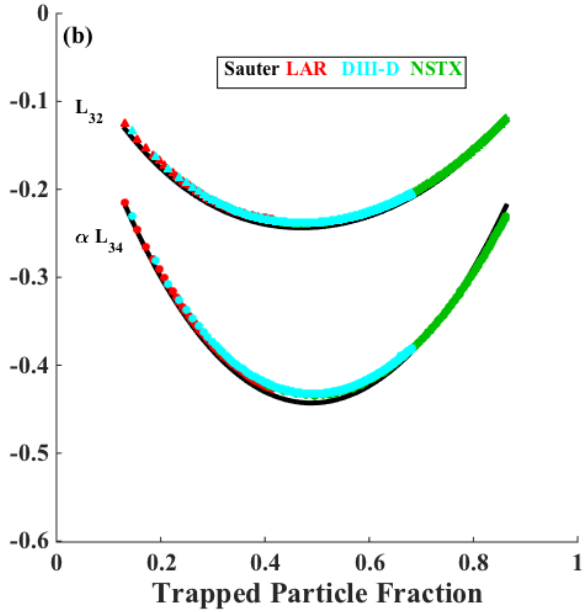

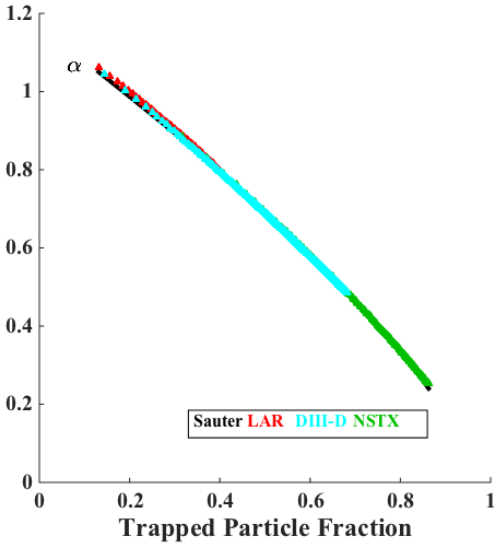

LAR & NSTX equilibria are from JSOLVER

Up-down asymmetric equilibria allow for the numerical evaluation of the geometric function Γ

$$\Gamma(\psi) = 2\frac{d}{d\psi}\oint d\ell\, \mathbf{B}\cdot\nabla R^2 + \oint \frac{d\ell}{B}\left[2\mathbf{b}\cdot\nabla\left(\nabla\psi\cdot\nabla \ln R^2\right)\right.$$
$$\left. +\nabla\psi\cdot\nabla(\mathbf{b}\cdot\nabla \ln B)\right]$$

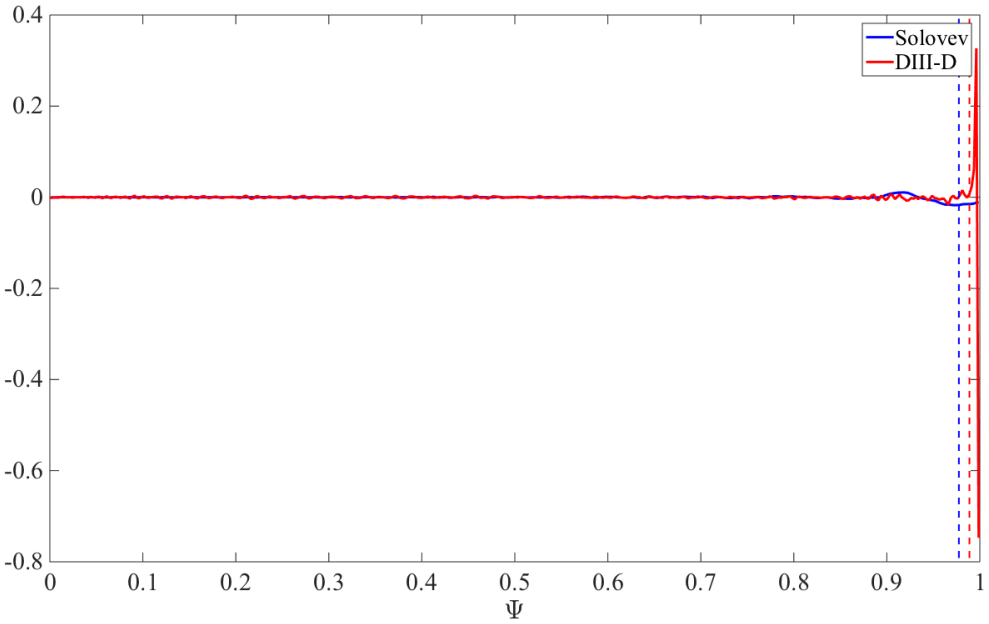

- Appears in ion DKE when $\nu_* \sim \delta \ll 1$
- Trivially zero for up-down symmetric equilibria
- Numerical evaluation within NIES from M3D-C^1 equilibria showed it to be small, albeit noisy
- Prompted further analytic evaluation, revealing it to be identically zero in all Grad-Shafranov equilibria

Summary and future work

- **NIES**
  - Now interfaces with M3D-C^1 axisymmetric equilibria, solving for
    - Steady-state, low-collisionality distribution functions
    - Neoclassical conductivity, poloidal flow, and bootstrap currents
  - Numerical evaluation and subsequent analytic evaluation of novel geometric factor present at extremely low collisionality has revealed it to be identically zero
  - NIES is therefore accurate in the $\nu_* \sim \delta \ll 1$ regime for both ions and electrons without further modification
- **DK4D**
  - Finite-collisionality, time-dependent DKE solver uses much of the same machinery that NIES uses
  - Should be able to interface with M3D-C^1 equilibria relatively easily
  - Will be used to provide neoclassical closure for M3D-C^1
  - Transport-timescale evaluation of axisymmetric steady-state equilibria with self-consistent resistivity and bootstrap currents

ADDITIONAL SLIDES

HFS q95 trends not captured by IPEC or MARS

IPEC

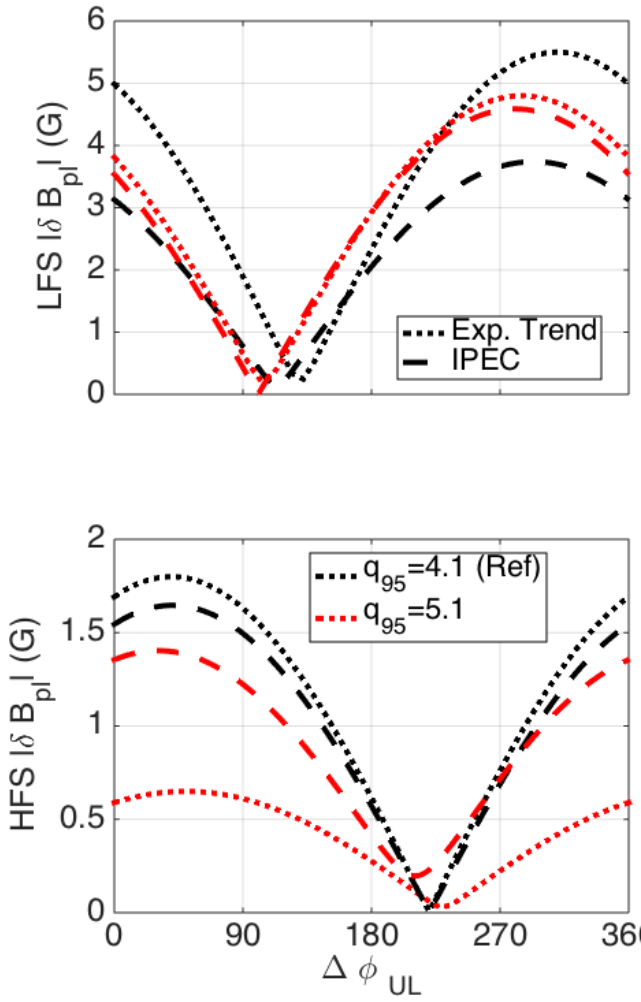

MARS-F

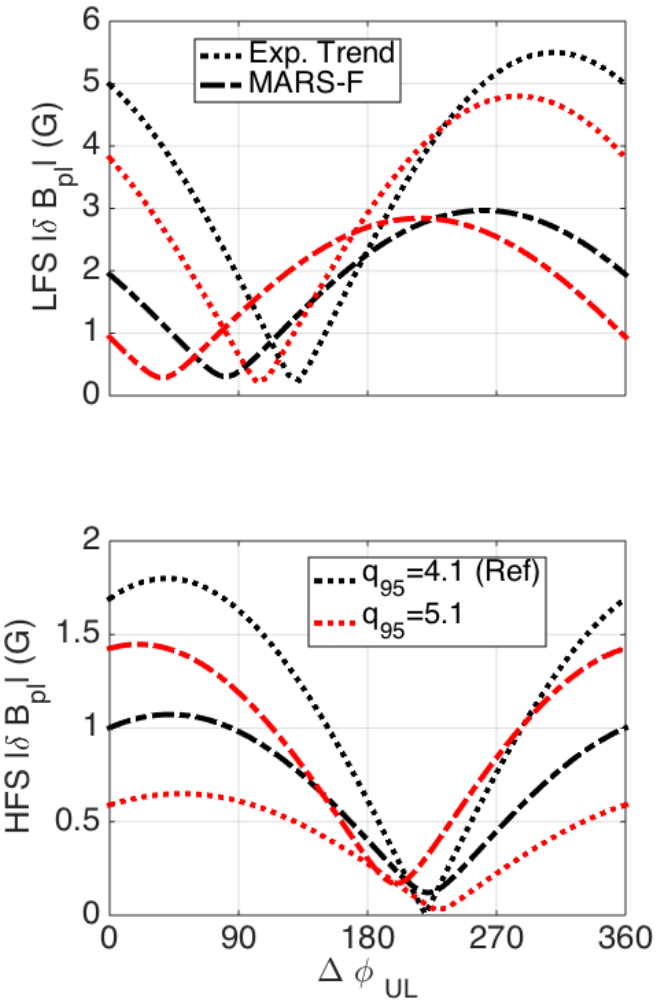

HFS H- to L-mode trends not captured by IPEC or MARS

IPEC

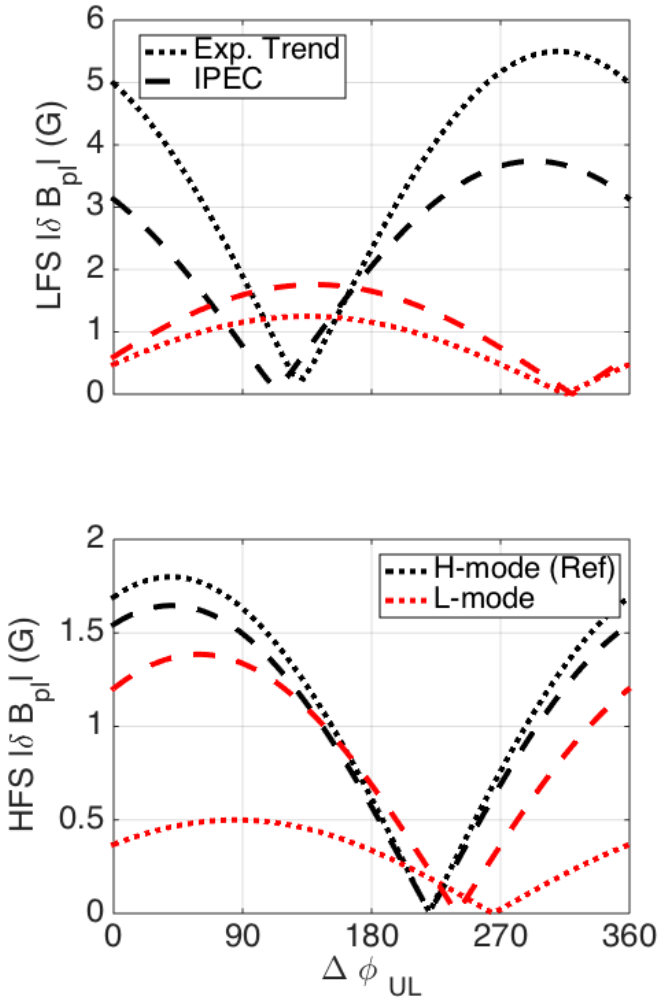

MARS-F

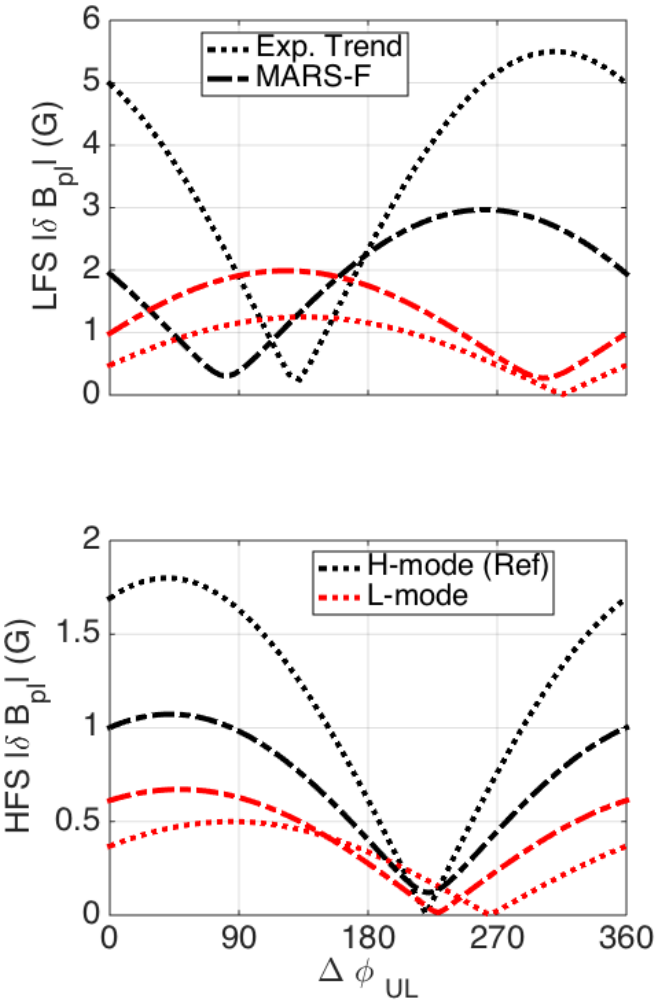

MARS-F agreement with L-mode data could be improved by using ExB rotation profile

Compared to M3D-C^1 using ExB rotation

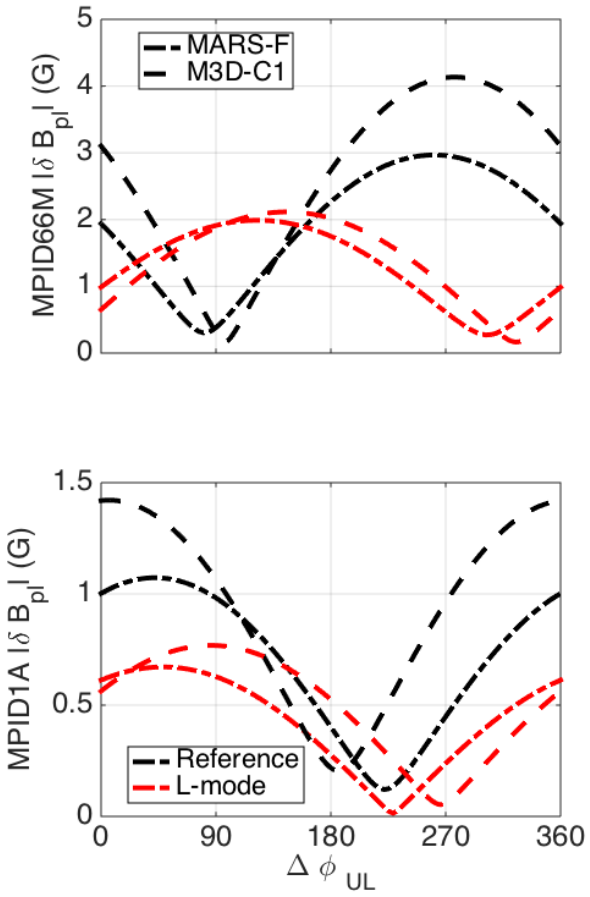

Compared to M3D-C^1 using carbon toroidal rotation

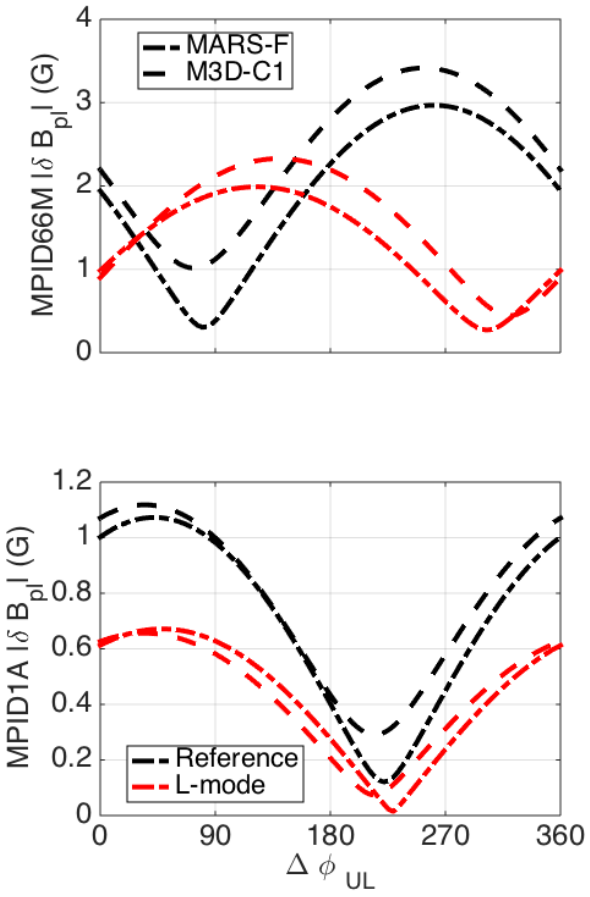

β trends are captured by IPEC for smoothly-varied equilibria, but not experimental reconstructions

VARYPED equilibria

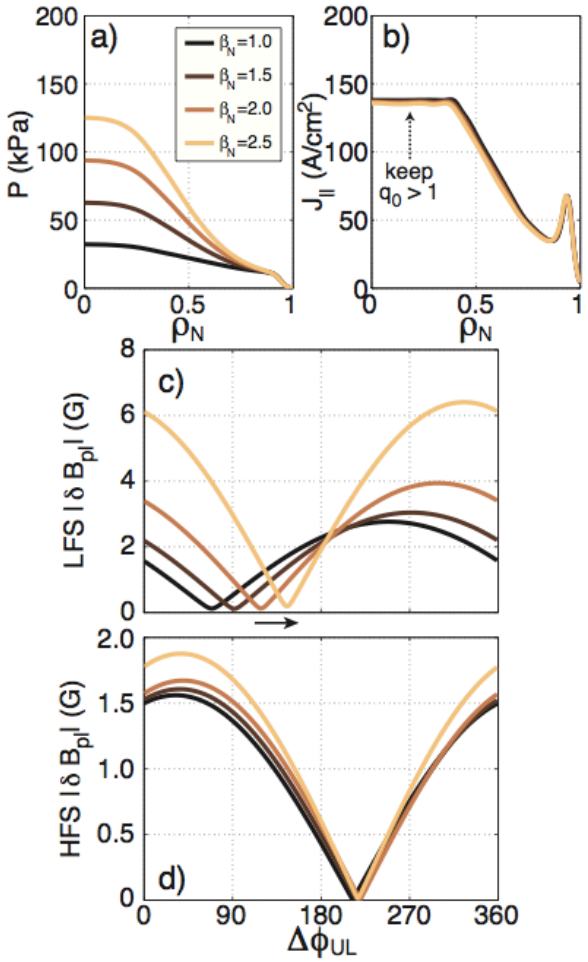

Experimental reconstructions